Soft Matter

PAPER

View Article Online
View Journal | View Issue

Check for updates

Cite this: *Soft Matter*, 2025, 21, 3757

What makes oil-in-water emulsions with pea protein stable? The role of excess protein in network formation and yield stress development†

Eleonora Olsmats, *[a] Adrian R. Rennie [a] and Daniel Bonn [b]

Received 23rd January 2025,
Accepted 9th April 2025

DOI: 10.1039/d5sm00082c

rsc.li/soft-matter-journal

Emulsions stabilized with pea protein exhibit enhanced stability only if excess protein is present in the continuous aqueous phase. We hypothesize that the additional protein, beyond the interfacial layer surrounding the oil droplets, is important for the emergence of a yield stress as well as for the overall stability and properties. Stable emulsions with oil concentrations of 40–60% v/v were prepared and compared to layers from various separated emulsions. Confocal microscopy visualized both the oil droplets and the protein distribution. Rheological measurements were used to assess mechanical properties and network formation. Small angle X-ray scattering provided quantitative structural information. Results identified that stable emulsions have a protein layer encapsulating the oil droplets and that excess protein forms irregular aggregates in the aqueous phase. Rheological analysis indicated that the protein aggregates contribute to network formation and give rise to a yield stress which enhances stability. Only for sufficiently high protein concentrations were the emulsions stable. Other samples separated and the upper phases were always similar in emulsion composition regardless of the initial component fractions. This study highlights the dual role of pea protein in emulsions as a dispersed protein network and as interfacial material. Determination of the most favourable emulsion composition provides insight into design of stable emulsions for applications.

Open Access Article. Published on 17 April 2025. Downloaded on 4/3/2026 5:41:20 PM.
This article is licensed under a Creative Commons Attribution 3.0 Unported Licence.

Introduction

Emulsions are metastable colloidal systems composed of two immiscible fluids, with one dispersed as droplets in a second continuous phase, finding applications in foods, pharmaceuticals, and industrial products.[1] While conventional low molecular weight surfactants are commonly used as stabilizers, increasing attention has been given to larger particles adsorbing at the interface. These particle-stabilized systems, known as Pickering emulsions,[2,3] offer potential as environmentally friendly alternatives to classic surfactant-stabilized emulsions and can provide enhanced stability.

Recent research has questioned the fundamental differences between surfactant-stabilized and Pickering emulsions, suggesting that the distinction may not be as clear-cut as previously thought.[4] This debate extends to protein-stabilized emulsions where the mechanism may involve elements of both traditional surfactant behaviour and that characteristic of particles. The complexity of protein adsorption and interaction at interfaces adds further intricacy to the understanding of these systems.

In the food and biomedical industries, there has been a shift towards using particles of plant origin to increase sustainability.[5] Proteins extracted from legumes such as soya beans, peas, and fava beans have gained attention due to their potential health benefits and ability to form stable emulsions. Pea proteins, rich in essential amino acids,[6] have been reported to provide good stability for emulsions at various pH values from 3 to 7,[7] both as aggregates acting as particle stabilizers[8–11] and as denatured individual protein molecules.[12] The mechanical properties and rheology of these materials attract major interest in new applications, such as 3D printing of food products.[13]

The stabilization mechanism in protein-based Pickering emulsions is complex and may involve multiple factors. The traditional view emphasizes the importance of particle size and wettability in determining the detachment energy of adsorbed particles[14] but recent studies suggest that protein-stabilized emulsions may exhibit behaviour characteristic of both particle-laden and molecular surfactant-covered interfaces.[4] This dual nature complicates the interpretation of stabilization mechanisms and challenges the conventional understanding of Pickering emulsions. Additionally, Dinkgreve *et al.* have studied

[a] *Macromolecular Chemistry, Department of Chemistry –Ångström, Uppsala University, Box 538, 75121 Uppsala, Sweden. E-mail: eleonora.olsmats@kemi.uu.se*
[b] *van der Waals-Zeeman Institute, Institute of Physics, University of Amsterdam, Science Park 904, 1018 XH Amsterdam, The Netherlands*

† Electronic supplementary information (ESI) available. See DOI: https://doi.org/10.1039/d5sm00082c

Open Access Article. Published on 17 April 2025. Downloaded on 4/3/2026 5:41:20 PM. This article is licensed under a Creative Commons Attribution 3.0 Unported Licence.

the mechanisms of clay particles as stabilizers and found that although emulsions showed good stability against coalescence while at rest, they quickly destabilized under shear.[15] Gel formation by clay particles in the continuous phase was crucial for stability rather than the clay particles simply being a good emulsifier. Whether this applies more widely to Pickering systems is still unclear.

Previous studies with pea protein identified stable emulsions in the range 30–60% v/v rapeseed oil and $>5\%$ w/v protein, where much of the protein is dispersed in the aqueous phase.[16] These samples were unchanged for periods of 7–14 days and structural studies provided insights into the arrangement of oil droplets and the interfacial protein layer. Small-angle X-ray scattering (SAXS) and quantitative fitting of data for emulsions with 40% v/v oil have revealed large emulsion droplets covered by a protein layer, identifiable as core-shell spheres, with excess protein in the bulk phase forming irregularly shaped aggregates.[16] However, the ambiguity in the model due to protein hydration makes it difficult to characterize the pea protein definitively as either individual interacting particles, as a polymer network, or both.

The requirement for an excess of protein beyond that needed to provide a monolayer around the oil droplets to form stable emulsions, challenges the notion that the Pickering mechanism of particles at the interface is the sole reason for the stability.[16,17] Recent work has suggested that the stabilization mechanism in protein-based emulsions may involve a combination of Pickering-like behaviour and traditional surfactant effects, with the relative contribution of each depending on factors such as protein concentration, pH, and ionic strength.[4] Even for small droplets of about 1 μm radius, the pea protein required to form a monolayer with 10–60% v/v oil is below 2.5% w/v, assuming a uniform 10 nm thick protein shell around monodisperse oil droplets. This discrepancy between the calculated amount of protein needed for monolayer coverage and the actual amount required for stability raises questions about the role of the excess protein that is present in the continuous aqueous phase. These systems may also be related to the oil-in-dispersion emulsions that have identified that dispersed particles in the aqueous phase can play an important role.[18]

To address these questions and to shed light on the nature of protein-stabilized Pickering emulsions, we investigate the role of excess protein in the continuous aqueous phase and discuss the differences between compositions of stable and unstable, phase-separated, samples. Our study combines microscopy, rheology, and small-angle X-ray scattering (SAXS) techniques to provide a comprehensive analysis of both stable compositions and those that separate into multiple layers, aiming to shed light on the complex stabilization mechanisms at play in these systems.

Experimental

Materials

Pea [*Pisum sativum* (L.)] protein was obtained from Superfruit Scandinavia AB (Växjö, Sweden), with a protein content of 83% w/w as provided by the manufacturer. The fat content, entirely unsaturated, was reported as 6.8% and the carbohydrate as insoluble fibre material as 5.3% w/w. The remainder is water and soluble salt. Rapeseed oil was supplied by Di Luca & Di Luca AB (Stockholm, Sweden). All other materials were of analytical grade. The *trans*-4-[4-(dimethylamino)-styryl]-1-methylpyridinium iodide (4-DASPI), and Nile Red were obtained from Sigma Aldrich (St. Louis, MO, USA).

Emulsion preparation and compositions

Stable emulsions were 40, 50 and 60% v/v rapeseed oil, 7.5% w/v pea protein and deionized water. Phase separating emulsions were 50, 40, 30, 20 and 10% v/v oil and 1 and 3% w/v pea protein. The compositions are described as the volume percentage of the oil and the water. The protein concentration is the percentage by weight in the total emulsion volume. All of the components were added separately. For the fluorescence microscopy experiments, the 4-DASPI was first dissolved in water and Nile Red in the oil prior to emulsification. A rotor-stator homogenizer D1000-M5, with 5 × 50 mm flat bottom probe (Benchmark Scientific Inc., Edison, NJ, USA) was used for sample preparation. Samples were prepared in 8 mL glass vials and homogenized for 1 min. Fresh samples were used for the experiments unless stated specifically. To check for stable or phase separated samples, they were left for 7 days of storage. The samples were at pH 7 which is well above the isoelectric point of pH 4.7 for the protein in water dispersions that was determined previously.[16]

Confocal microscopy

Microscopy analysis of the emulsions was conducted using a Leica TCS-SP8 confocal laser scanning microscope equipped with a 100× magnification oil immersion objective. Nile red, which was used to stain the oil dispersed phase, has an absorption maximum at 559 nm and an emission maximum of 635 nm. A laser with wavelength 552 nm was used for the excitation and an emission range of 580–700 nm was chosen. Although, 4-DASPI has mostly been used with polymer solutions,[19] it is known to associate to pea protein.[20] It was used as a fluorescence probe in the aqueous phase and it has absorption and emission maxima at 488 nm and 600 nm, respectively.[21,22] A laser with wavelength 488 nm was used for excitation and an emission range of 500–700 nm was used for those measurements. To avoid possible spectral interference during the fluorescence imaging, samples were prepared separately with one dye at a time. These dyes were chosen as they have been used for previous experiments with this system.[17,20] Quantitative analysis was performed using the Leica Application Suite X (LAS X)[22] and ImageJ[23] software platforms.

Rheology

Rheological behaviour of the pea protein emulsions was measured using an MCR301 rheometer (Anton Paar, Austria) with a rough cone plate geometry (CP 50-1) at 20 °C. Oscillatory and continuous rotation measurements were performed following the protocols summarized in Table 1. Briefly, creep rheology measurements with various constant applied stresses, τ, are presented in plots of shear rate *versus* time. Flow curves of

 This journal is © The Royal Society of Chemistry 2025

Table 1 Rheology measurement protocols

Measured properties	Reported results	Pre-shear treatment	Measuring protocol
Flow curve	Fig. 3	$\dot{\gamma}$: 500 s^{-1} for 30 s	1. $\dot{\gamma}$: 1000 to 0.01 s^{-1} during 100 s
Viscoelastic properties (protein network formation) with time	Fig. 4	$\dot{\gamma}$: 500 s^{-1} for 30 s	1. γ: 1%, ω: 1 rad s^{-1} for 100 s and 5000 s 2. γ: 0.1 to 1000%, ω: 1 rad s^{-1} during 100 s
Yield stress fluid behaviour	Fig. S5 (ESI†)	$\dot{\gamma}$: 500 s^{-1} for 30 s rest for 30 s	1. τ: 0.01–100 Pa as indicated in Fig. S5 (ESI†)

Open Access Article. Published on 17 April 2025. Downloaded on 4/3/2026 5:41:20 PM. This article is licensed under a Creative Commons Attribution 3.0 Unported Licence.

shear stress *versus* shear rate, $\dot{\gamma}$ were measured as quick sweeps from high to low shear rates. Strain amplitude sweeps show the storage and loss moduli as a function of shear stress. The purpose of the creep and flow curve measurements was to explore the yield behaviour of the emulsions over time. The creep measurements looked at the behaviour over long times (hours), whereas the flow curve measurements were performed as quick scans over shorter times (minutes). The amplitude sweeps were performed to study the dynamics of the formation of a protein network within the bulk phase. All measurements were made on samples shortly after preparation and the pre-shear treatment shown in Table 1. The Herschel–Bulkley model is used to fit the flow curve data and is described by

$$\tau = \tau_y + \kappa\dot{\gamma}^n \quad (1)$$

where τ is the shear stress, τ_y is the yield stress, κ is the consistency, $\dot{\gamma}$ is the shear rate and n is the flow index.

Small/ultra-small angle X-ray scattering (SAXS/USAXS)

SAXS data were collected on the Xeuss 2.0 Q-Xoom instrument (Xenocs, Grenoble, France) at Uppsala University, Sweden. An X-ray beam of wavelength λ = 1.54 Å was produced by the Genix3D Cu K_α microfocus source with integrated mirror optics and the scattered intensity was measured with a Pilatus 3R 300k detector (Dectris, Switzerland). The sample to detector distance was 2400 mm and the samples were mounted in circular holder with diameter ~2.5 mm and Kapton windows. The sample thickness was about 1.5 mm and the temperature kept at 22 °C. The collimation system was set by apertures of 0.7 × 0.7 mm near the source and 0.4 × 0.4 mm closer to the sample. The measurement times were 60 min. The XSACT software[24] was used for data reduction, including masking bad pixels, azimuthal averaging and background subtraction of measurement of an empty holder with Kapton windows.

The USAXS measurements were performed in the Bonse–Hart configuration on the same instrument as described previously and with similar environment. A Bartels channel-cut silicon monochromator and a 4-bounce channel-cut silicon analyser, both diffracting from (111) crystal planes, were added. The apertures were set to 3.0 × 3.0 and 1.4 × 1.4 mm to allow for a higher flux, however the measurement time was extended to roughly 4 h to obtain a good signal.

The data are presented in plots of the logarithm of scattered intensity, I, *versus* the logarithm of momentum transfer, Q, defined as

$$Q = \left(\frac{4\pi}{\lambda}\right)\sin\left(\frac{\theta}{2}\right) \quad (2)$$

where θ is the scattering angle and λ is the wavelength. The intensity of the SAXS data is placed on an absolute scale by normalizing the scattering to that of the transmitted direct beam. This has been checked by comparison to a sample of glassy carbon.[25] The intensity of the desmeared USAXS data was scaled to the SAXS data over the common data range with scale factor 1 × 10^5.

Results and discussion

Stable compositions with 7.5% protein

Confocal microscopy. The microstructure of emulsions was observed by confocal microscopy to examine the distribution and arrangement of both oil droplets and protein within the continuous aqueous phase. Fig. 1(a) and (b) show representative images of oil and protein labelled emulsions. The temperature colour scale from black to blue is used to represent the intensity. As seen readily in the images, there is oil droplet formation (Fig. 1(a)) and protein dispersed in the continuous water phase as individual particles (Fig. 1(b)). A layer of protein at the interface of the bigger oil droplets is also observed.

Images for a series of emulsions with different oil fractions are shown in Fig. 2 for each fluorescent label. The oil is visualized with Nile Red (Fig. 2(a)–(c)) and the protein location is determined from staining the pea protein with 4-DASPI (Fig. 2(d)–(f)). The emulsions were measured within one hour of preparation after the homogenization treatment to provide observations without significant ageing. Emulsions with 7.5% w/v pea protein and 40, 50 and 60% v/v oil are shown. The droplet size is slightly larger for lower oil fractions (Table 2).

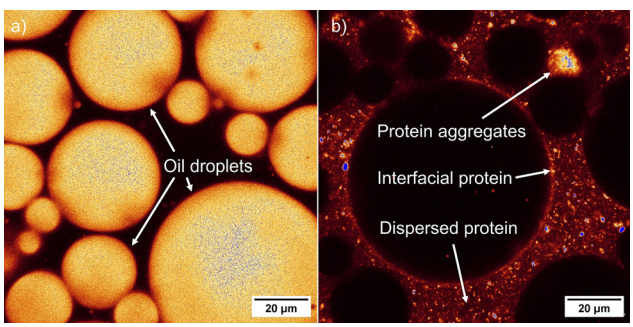

Fig. 1 Representative images of oil-in-water emulsions stabilized with pea protein. (a) The oil is fluorescently labelled. (b) The protein is fluorescently labelled. The intensity is indicated by a temperature colour scale. The scale bars in the lower right corners of each image are 20 μm. These images are taken from the creamed phase of separating emulsions that are described further below.

Open Access Article. Published on 17 April 2025. Downloaded on 4/3/2026 5:41:20 PM.
This article is licensed under a Creative Commons Attribution 3.0 Unported Licence.

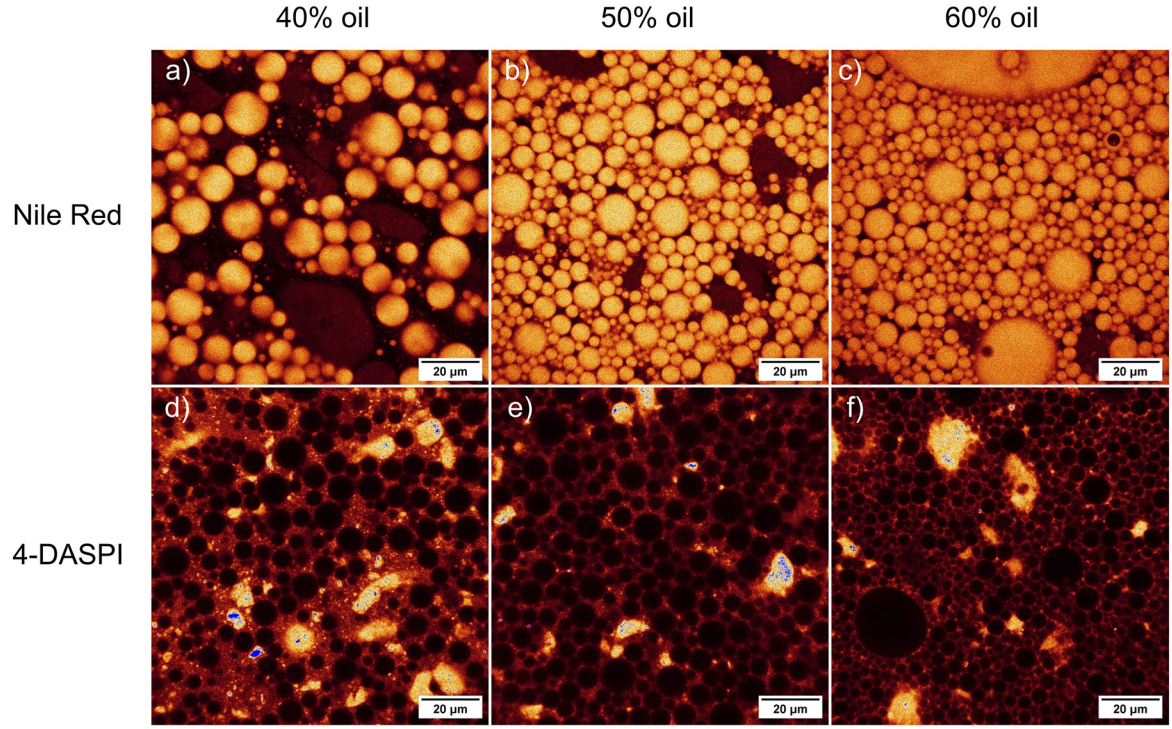

Fig. 2 Confocal micrographs of emulsions stabilized with 7.5% w/v pea protein. The emulsions are stained with Nile Red (a)–(c) in the oil, and 4-DASPI attached to the protein (d)–(f), respectively. The oil content is 40% v/v (a) and (d), 50% v/v (b) and (e) and 60% v/v (c) and (f) and the mean droplet radii are 3.5, 2.4 and 2.3 μm for the different oil fractions, respectively. The scale bars in the lower right corners of each image are 20 μm.

Table 2 Mean droplet radius of stable emulsions after preparation and after 7 days of storage at 19 °C. One standard deviation of the size distribution is indicated by ± and histograms of the radii are presented in Fig. S4 in the ESI†

Oil concentration / % v/v	Pea protein concentration / % w/v	Mean droplet radius of fresh emulsions / μm	Mean droplet radius after 7 days / μm
40	7.5	3.5 ± 1.3	3.5 ± 2.1
50	7.5	2.4 ± 1.3	2.6 ± 1.6
60	7.5	2.3 ± 1.4	1.5 ± 0.8

Description of the calculations of droplet size is provided in Section S1 in the ESI.† The result is surprising, as the decrease in surface area as a combined effect of the lower oil fraction and the bigger droplets would require less material to be present at the oil/water interface. The phenomenon of bigger droplets at higher oil fractions has been reported previously for oil contents 10–80%. Li *et al.*[10] and Mota da Silva *et al.*[26] used low protein content of less than 1%, which would be expected to almost entirely adsorb at the surface of the droplets and that could explain the increase in droplet size for high oil fractions. Zhan *et al.*[27] and Shao *et al.*[8] used higher protein content of 2–5%, which is expected to provide a slight excess to that present as a thin layer at the interface. However, the high protein content of 7.5% w/v in the emulsions studied is considerably in excess of that expected to be needed to cover the droplet surface. We will further discuss the role of the protein. Our microscope images suggest that the protein forms a gel-like structure in the continuous phase with regions of higher intensity due to clusters or larger connected aggregates of protein. The larger droplets at the lower oil concentrations in our study can be explained by the decrease of pea protein concentration in the aqueous phase. As the protein does not disperse in the oil, the concentration in the aqueous phase decreases significantly with lower oil fractions. The dense protein network entraps the oil droplets, and prevents rapid coalescence. We observe that the protein in the bulk phase in addition to the layer at the interface is necessary for the formation of stable emulsions. Not surprisingly, broad droplet size distributions were seen for all samples. This has been reported frequently in previous studies.[16,28–31] In order to investigate the effects of aging, emulsion compositions were chosen that corresponded to visually stable emulsions after 7 days storage at room temperature as in our previous study.[16] Confocal microscopy images after 7 days of storage at room temperature are shown in Fig. S1 (ESI†) and these confirm the earlier stability studies. No changes in droplet size, and location or aggregation of the protein were observed after storage. Comparative analysis of Fig. 2 and Fig. S1 (ESI†) are reported in Table 2 and the size distributions are given in Section S1 in the ESI.†

Interestingly, protein dispersed in the aqueous phase is the dominant feature in the images in Fig. 2(d)–(f), where the pea protein is stained with 4-DASPI. We see some of the material present at the surface of oil droplets and the surface-active behaviour of pea protein has been reported previously from

 This journal is © The Royal Society of Chemistry 2025

Open Access Article. Published on 17 April 2025. Downloaded on 4/3/2026 5:41:20 PM.
This article is licensed under a Creative Commons Attribution 3.0 Unported Licence.

measurements of interfacial tension.[32–34] For 40–60% v/v oil emulsions with small 1 μm radius and a 10 nm protein film at the interface, the protein concentration required is 1.5–2.2% w/v. However, for droplet radii of 3 μm, these numbers are reduced to 0.49–0.74% w/v. We have considerably more protein in the emulsions, where the excess is dispersed in the aqueous phase.

Rheology. The high protein content in the bulk phase observed in the micrographs and reported previously from analysis of X-ray scattering[16] is interesting from a rheological perspective. One observation from the confocal microscopy of the stable emulsions is the dense network of protein particles within the bulk phase, which could influence the rheological behaviour. Rheological measurements have been used to study the influence of protein networks within the bulk phase on flow behaviour of the emulsions.

The flow curves for the emulsions with plots of applied stress against shear rate indicate yield stress fluid behaviour. Yield stresses for samples with 7.5 and 15% w/v pea protein in water and 40, 50 and 60% v/v oil emulsions were determined from the flow curve experiments and the corresponding Herschel–Bulkley (eqn (1)) model fits where appropriate. These are presented in Fig. 3(a). The parameters for the fits are presented in Table S1 in the ESI.† The existence of a yield stress at rest is easily demonstrated by the inverted vial test[35] as seen in Fig. 3(b) and (c). Directly after preparation, the emulsions with a lower oil fraction have a low viscosity and do not exhibit a yield stress in the inverted vial test, so if they have a yield stress it is smaller than that of the gravitational field. Further, after storage for 5 days in an upright position, the inverted vial test indicates a yield stress fluid behaviour also for the lower oil content emulsions, suggestive of network formation over time. The presence of a yield stress at lower oil volume fractions than the random close packing of 0.64 also suggests that the network of dispersed protein is important: an emulsion with purely repulsive drops only exhibits a yield stress above this volume fraction. The significance of a yield stress within the continuous phase for emulsion stability has been discussed previously by Dinkgreve *et al.* for clay stabilized emulsions[15] using a swelling clay[36] and there are clear similarities with our system. Dinkgreve *et al.* showed that oil drops can be stabilized within a yield stress material but as soon as the emulsion starts to flow, the drops touch and coalesce.

In our system, for a dispersion of 7.5% w/v pea protein alone in water, no yield stress was observed, but for a higher protein concentration of 15% w/v corresponding to the effective concentration in the aqueous phase for a 50% v/v oil emulsion, a yield stress was present. The parameters for the Herschel–Bulkley model fits are presented in Table S1 (ESI†). The observation of a yield stress for high protein content dispersions in water (without the dispersed oil phase) helps the understanding of the role of the high protein concentration in the aqueous phase to increase emulsion stability. It also explains the observations from the confocal micrographs that larger droplets at lower oil fractions are due to less entrapment of oil droplets in a looser protein network.

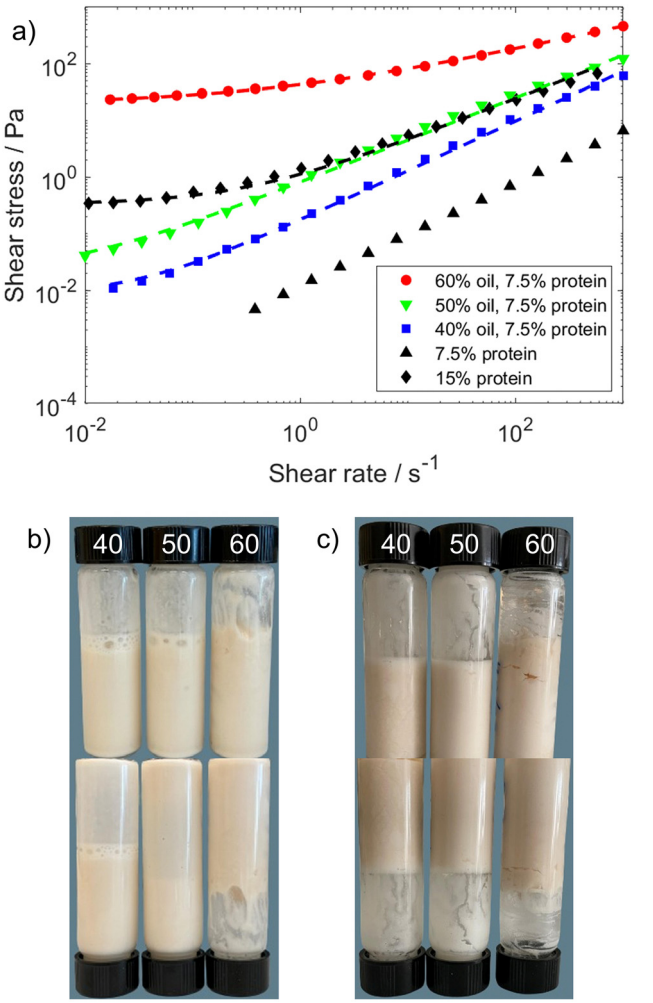

Fig. 3 (a) Flow curves for emulsions with 40, 50, 60 and 0% v/v oil, and 7.5 and 15% w/v pea protein. The dashed lines are the fitted Herschel–Bulkley models (eqn (1)) with parameters in Table S1 (ESI†). (b) Inverted vial test after preparation. (c) Inverted vial test after 5 days of storage at 19 °C. The samples from left to right are made with 40, 50 and 60% v/v oil and 7.5% w/v pea protein.

Additional creep measurements to demonstrate the yield stress behaviour are presented in Fig. S5 in the ESI.† The shear rate decreases below a particular applied stress, the yield stress, which indicates that the system ages, a hallmark of thixotropic yield stress materials.[37] All this confirms the observation from confocal microscopy images of protein interacting in the bulk phase and opposes the idea of a single mechanism with Pickering stabilization. While the absolute value for the yield stress should not be overanalysed due to the complexity and polydispersity of the systems, it is interesting to investigate the time dependent yield stress.

Further experiments, to study the time dependence on the emulsion behaviour and the formation of a particle network in the bulk phase, were performed as strain amplitude sweeps after different times. Fig. 4(a) shows data for a strain amplitude sweep from 0.1 to 1000% after 100 s of sample at 1% strain and 1 rad s^{-1} frequency and Fig. 4(b) shows the amplitude sweep

Open Access Article. Published on 17 April 2025. Downloaded on 4/3/2026 5:41:20 PM.
This article is licensed under a Creative Commons Attribution 3.0 Unported Licence.

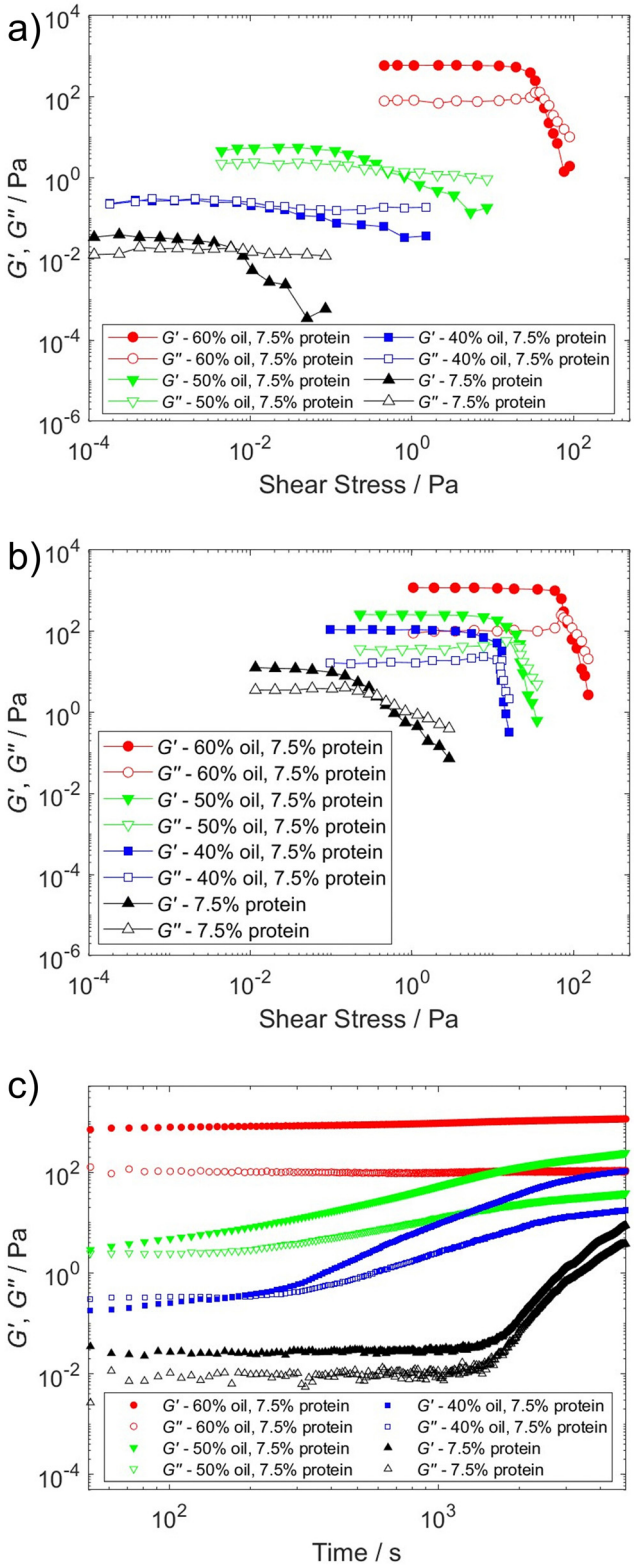

Fig. 4 (a) Amplitude sweep after 100 s of shear. (b) Amplitude sweep after shear for 5000 s. (c) G' and G'' responses with time.

after 5000 s at 1% strain and 1 rad s^{-1} frequency. The change in viscoelastic behaviour is interesting: the storage and loss modulus (G' and G'') increase with time and with increasing oil concentration both G' and the crossover stress where G' and G'' intercepts are shifted to higher values as shown in Fig. 4(c); they show a rapid upturn in G' and G'' at times of several hundreds or thousands of seconds. These effects are more pronounced for the samples with lower oil content and for the dispersion of pea protein in water. G' is greater than G'' at rest and G' increases with time, which again suggests that these systems are thixotropic yield stress fluids.

A caveat concerning the rheological results presented in Fig. 4(c) is that at long times there are likely to be some effects of drying of the samples. To quantify an upper limit for the degree of evaporation that could be expected, samples were placed in an open environment and the weight was monitored over time as seen in Fig. S6 (ESI†). During the first 5000 s, corresponding to the measurement time in the rheological study, the upper boundary for the weight loss of the emulsions was 13–16%. The significantly higher rate of evaporation for the 7.5% w/v pea protein dispersion in water as compared to the emulsions and 15% w/v protein dispersion may be due to small fractions of surface-active material. The aqueous phase in the emulsions corresponds approximately to the more highly concentrated dispersion. It is difficult to quantify exactly how much impact the drying process has on the rheological measurements but as observed in Table S2 (ESI†), the changes in G' and G'' are significantly larger than those that can be attributed solely to the change in concentration due to evaporation.

Compositions that separate into stable emulsions

Confocal microscopy. An intriguing observation is that when there is insufficient protein to form a bulk stable emulsion, the system phase separates into an aqueous phase at the bottom, and an emulsion phase at the top. This separation is sometimes accompanied by a layer of sedimented protein at the bottom that is in excess of that required for the separated layer of stable emulsion. To obtain a better understanding of the conditions under which emulsions form, a comparison of the bulk stable emulsions was made with the phase-separated layer in the separated samples. Fig. 5(b) and (c) show samples with 10–50% v/v oil stabilized with 1 and 3% w/v pea protein, respectively, after 48 h of storage at 19 °C. Confocal microscope analysis was performed on the upper oil-rich phase and the middle aqueous phase separately. The images with Nile Red as fluorescent dye are shown in Fig. 6 (upper phase) and Fig. S7 (middle aqueous phase) in the ESI.† The results with 4-DASPI as the dye for the protein are presented in Fig. S12 (upper phase) and Fig. S13 (middle aqueous phase) in the ESI.† Interestingly, the upper, creaming phases show similar compositions of 34–64% oil (see Table S3 in the ESI†) despite the different original component fractions. This composition is similar to the range of bulk stability of 30–60% v/v oil that was reported in our previous work.[16] The droplet size was found to be in the range 5–12 μm. The pea protein concentration in this phase is larger than 3% w/v, which also corresponds well with the region of stability of 5–17% w/v pea protein reported earlier.[16] Confirmation of the composition in the samples was made by measuring the density of the different layers in the

 This journal is © The Royal Society of Chemistry 2025

Open Access Article. Published on 17 April 2025. Downloaded on 4/3/2026 5:41:20 PM.
This article is licensed under a Creative Commons Attribution 3.0 Unported Licence.

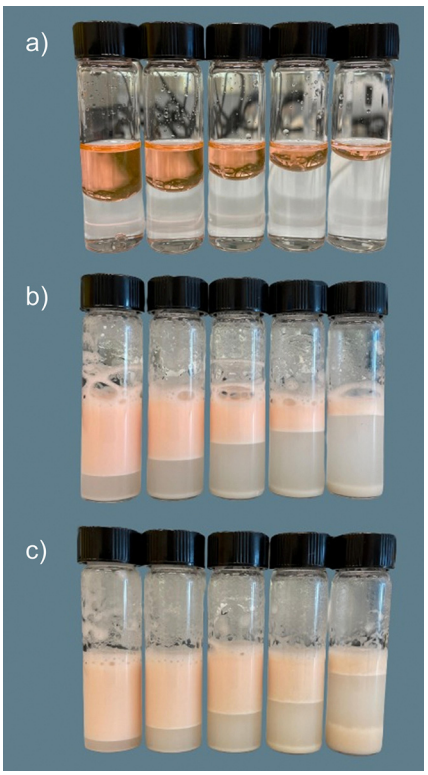

Fig. 5 Samples from left to right with 50, 40, 30, 20 and 10% v/v oil. (a) Oil and water fractions without protein. (b) Phase-separated emulsions with 1% w/v pea protein. (c) Phase-separated emulsions with 3% w/v pea protein. The pictures were taken after 48 h of storage at 19 °C.

phase separated samples. The data are shown in Fig. S14 in the ESI.† The droplet size was seen to be smaller for the samples with the pea protein concentration of 3% than for 1%. This is not unexpected as the presence of more pea protein which is a surface-active material favours the creation of more interface. The formation of a creaming layer with similar compositions that are independent of the starting oil fraction, suggests that the stability for this system is strongly favourable for oil fractions around 50%. This is a promising result for product development and food applications as a state of thermodynamic stability for a particular composition poses less constraints on the preparation method and homogenization quality. With a sufficiently high concentration of pea protein present in the aqueous phase, the network formation and yield stress are enhancing stability, making it highly suitable for long storage. The full description of the droplet analysis is provided in Section S4 in the ESI.†

Small/ultra-small angle X-ray scattering (SAXS/USAXS). To further understand the microstructure and its implications for stability of the different phases in unstable emulsions, USAXS and SAXS techniques were used. Scattering data for the different phases in separated samples with 10–50% v/v oil were collected and are shown in Fig. 7. The upper creaming phases all show broadly similar patterns in the low Q region in Fig. 7(a) that is attributed to the presence of larger scattering entities such as oil droplets and the protein as described previously.[16,17] These findings confirm the observations from the fluorescence microscopy images which indicate that the creaming phases have similar compositions and droplet size distributions regardless of the initial oil fraction. Data for a stable emulsion with 50% v/v oil and 7.5% w/v pea protein have been added as a reference and show significantly higher intensity. The higher intensity corresponds to the smaller droplet radius as observed in confocal microscopy in Fig. 2(b) compared to Fig. 6. The increased surface area of the smaller droplets enhances the scattering intensity in this range of small Q. Even greater

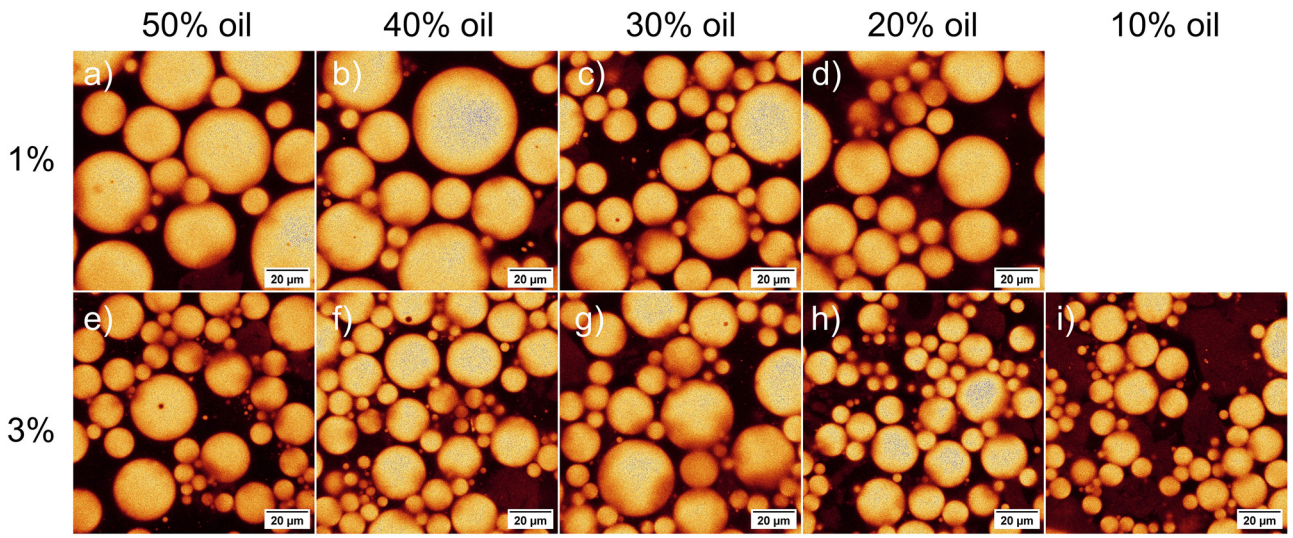

Fig. 6 Confocal micrographs of the upper creaming phase of separated emulsions after 48 h of storage at 19 °C, stained with Nile Red. The emulsions are stabilized with 1% (a)–(d) and 3% (e)–(i) w/v pea protein, respectively. The oil content for the original emulsions from left to right is 50, 40, 30, 20, 10% v/v. The sample with 10% oil and 1% pea protein did not produce enough creaming phase to be analysed in this experiment. The mean droplet radii are (a) 12, (b) 10, (c) 7.4, (d) 8.9, (e) 7.0, (f) 6.6, (g) 7.5, (h) 5.5 and (i) 5.0 µm. The scale bars in the lower right corners of each image are 20 µm.

Open Access Article. Published on 17 April 2025. Downloaded on 4/3/2026 5:41:20 PM.
This article is licensed under a Creative Commons Attribution 3.0 Unported Licence.

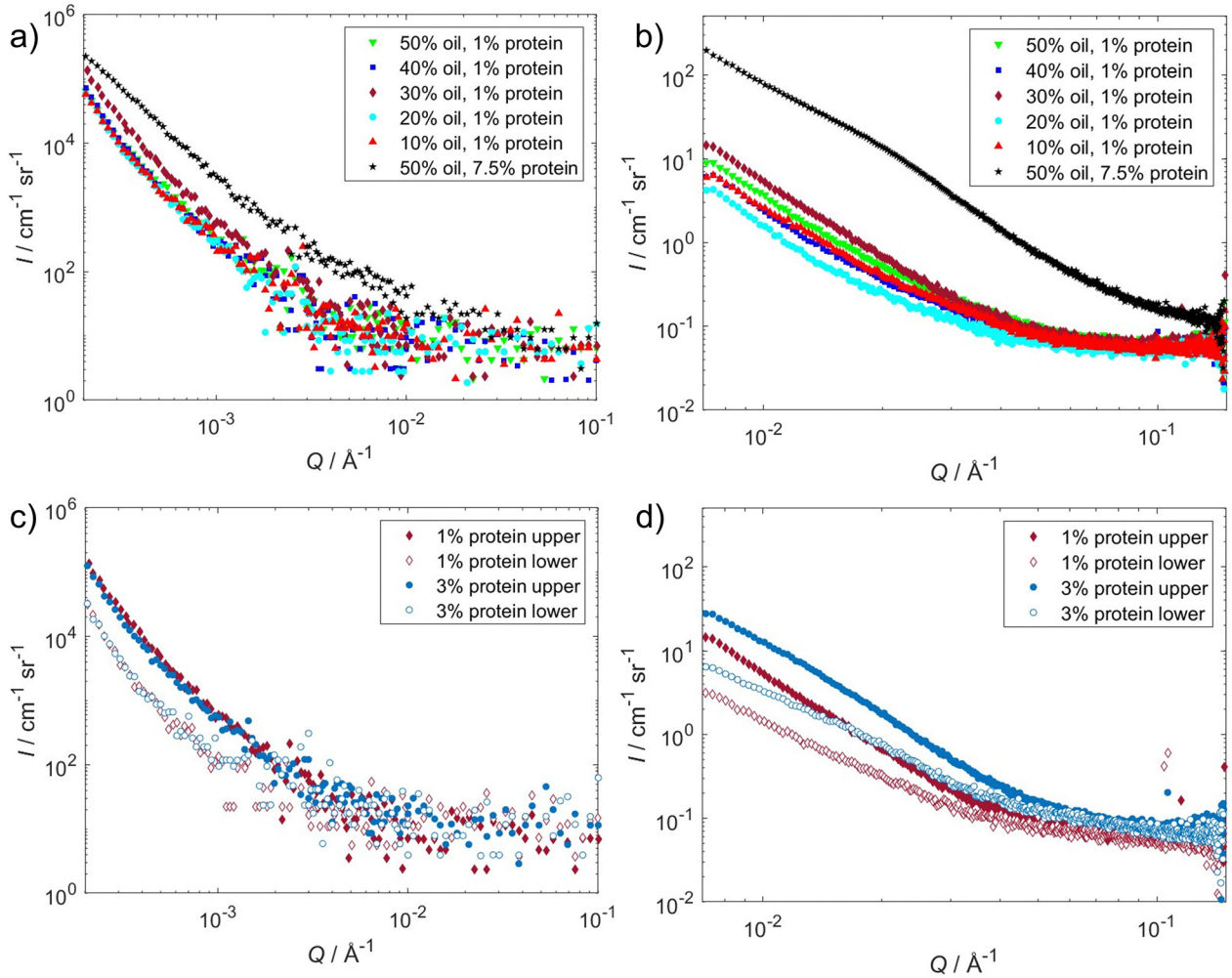

Fig. 7 (a) USAXS data for the upper creaming layer of separated emulsions. The original compositions in the emulsions before separation are 1% w/v pea protein and 10–50% v/v oil. Data from a stable emulsion with higher protein content for 7.5% w/v pea protein and 50% v/v oil are added as a reference. (b) SAXS data for the same samples. (c) USAXS data for the upper creaming layer and lower aqueous layer of separated emulsions. The original compositions in the emulsions before separation are 1–3% w/v pea protein and 30% v/v oil. (d) SAXS data for the same samples.

differences in scattering patterns are noted at higher Q values in Fig. 7(b). These differences are primarily due to the dispersed protein in the continuous phase and is not a surprising result. The excess protein in highly concentrated pea protein emulsions predominantly resides in the continuous phase as evidenced by the microscopy images (Fig. 2(e) and Fig. S12 in the ESI†).

When comparing the scattering patterns from samples with starting compositions of 1 and 3% w/v pea protein and 30% v/v oil in Fig. 7(c), the results show no significant differences in the low Q range. However, a clear differentiation exists between the bottom aqueous phases and the top creaming phases. The bottom phases consist mainly of water, with small amounts of protein and oil, whereas the upper creaming phases consist of micrometre-sized droplets and proteins both at the droplet surface and dispersed within the aqueous phase. These findings suggest that, within the resolution limits of the scattering measurements, a consistent droplet size and concentration are recorded within the creaming phase as was also seen in the confocal microscopy images in Fig. 6. The difference in intensity in Fig. 7(d) between the samples are linked to the amount of pea protein in the continuous phase. Samples with higher pea protein concentrations of 3% exhibit greater scattering intensity due to the higher availability of excess protein in the continuous phase.

Even with simple qualitative analysis of the scattering data, the USAXS/SAXS results give a clear confirmation of the observations from the confocal microscopy images that unstable compositions separate into layers that have similar composition and structure as stable emulsions. A protein content of a few percent, oil fractions around 50% v/v, and droplet radii 5–10 μm in the top phase are shown to be formed favourably at equilibrium under storage.

Overall discussion

The rheological measurements indicate that the role of the dispersed protein in the bulk phase is important in the creation of a time-dependent gel-like structure in the continuous phase.

 This journal is © The Royal Society of Chemistry 2025

Open Access Article. Published on 17 April 2025. Downloaded on 4/3/2026 5:41:20 PM. This article is licensed under a Creative Commons Attribution 3.0 Unported Licence.

The results suggest that individual constituents of pea protein particles and molecules of different sizes interact and act to induce an effective attraction between the oil droplets. This effective interaction potential together with the protein network in the continuous phase leads to the observation of a yield stress at concentrations of oil below the critical packing fraction for spheres. Pea protein gels have been studied previously by Zhang *et al.*[38] They saw gel formation ($G' > G''$) with 10–15% w/v protein after high pressure homogenization at 300 and 600 MPa. The protein content in that investigation is similar to that which we have identified as necessary to be present in the aqueous phase of the emulsions for stability. It is probable that the homogenization process during emulsion preparation is enough to enhance the exposure of internal hydrophobic groups and free sulfhydryl groups, which promotes aggregation and gel formation. Although the study by Zhang *et al.*[38] reported a fine-stranded and smooth gel at pH 7 dominated by hydrogen bonding, at pH 5 close to the isoelectric point, they reported hydrophobic interactions as the dominant mechanism for the creation of a compact gel structure where distinct particles or clusters of protein molecules were present. Also, the study by Chen *et al.*[39] showed a coarse pea protein network with strands and large aggregates as big as several hundred nanometres and a less continuous and heterogeneous network than those found for many other materials such as those produced by whey proteins. They were able to identify individual nano-sized spherical or ellipsoidal particles as the constituents in the network by microscopy and small angle scattering studies. It should be noted that their study used 13% w/w pea protein in water however, it mostly considered the effect of heating on the gelation process rather than changes at ambient temperatures. It is likely that the effect of the protein in the bulk phase is similar to that in the present studies as seen in the confocal microscopy images and the rheological results in the various studies of pea protein gels.[38,39] However, the network in present study is likely to be composed of different size protein molecules and protein aggregates rather than consisting of a uniform polymeric gel. The time dependence of G' and G'' suggests that structural changes in the dispersed protein are significant. The high protein content in the emulsions, in excess of that needed to create a monolayer of absorbed protein molecules at the interface, shows that the protein is not only located in a layer around the droplets but also dispersed in the continuous phase. There is still work necessary to distinguish whether particular components are present at the interface and in the bulk aqueous phase, although some insight can be gained from previous studies.[32,40,41] The emulsions with compositions of 40–60% v/v oil and 7.5% w/v are shown to be stable after storage. Emulsions with this range of oil fractions are also seen to form in the creaming layer of phase separated samples, independent of the initial composition for samples with less protein (1 and 3% w/v) and lower oil fractions (10–50% v/v). This is due to the emergence of a yield stress above a critical gel forming protein concentration in the aqueous phase. The assembly to an equilibrium creaming phase with large and stable emulsion droplets has potential for applications, as thermodynamically stable systems open new pathways to product materials. This could be a route to defined compositions with exceptional stability due to the additional stabilization of entrapped droplets in a network or viscous matrix. The equilibrium state is an important finding in the use for pea protein stabilized emulsions in industrial settings, as this puts less requirements on the preparation method and homogenization quality. It is interesting to compare this observation to the stable Pickering emulsions and particle-stabilized nanoemulsions where stable phases form spontaneously on gentle mixing without significant extra applied energy.[42,43] However, the droplet size for these systems are considerably smaller and less polydisperse. The extension of such behaviour to larger droplets that use food grade materials is an important result for applications.

Conclusions

The results complement previous studies[16] that identified that stable emulsions with rapeseed oil, water and pea protein are formed with oil volume fractions in the range 30–60% v/v and that a large amount ($>5\%$ w/v) of pea protein was necessary. The stable samples were unchanged for periods of 7–14 days. This work showed that compositions with more water are unstable and display creaming within about an hour. The creamed phase was identified as forming the same composition as a stable emulsion prepared with 50% v/v water. This gives an appearance of good kinetic stability. Slow phase separation or kinetic stability could be a consequence either of gelation or the presence of large stabilizers such as Pickering particles. The apparent fixed composition is however unusual. The stability is clearly not arising solely from particles at the oil–water interface as occurs in Pickering emulsions.

The role of the protein is interesting as it apparently interacts in two major ways. Confocal microscopy clearly identifies particles of protein in the continuous aqueous phase as well as at the surface of the oil droplets. This was confirmed with X-ray studies. Studies of rheology show that the emulsions have a yield stress even below the maximum packing fraction. The yield stress is also present for samples of the protein alone dispersed in water. This indicated that a network was formed. Confocal microscopy shows clusters of oil droplets that could also be part of a gelled network. An explanation of this aspect of the behaviour would be that the dispersed protein in the aqueous phase acts as a depleting agent. This is apparently similar to the behaviour of another system, a high internal phase emulsion, that was prepared with LAPONITE® particles.[15] Above a critical gel forming protein concentration in the aqueous phase, the emergence of a yield stress clearly enhances the stability. This also contributes to the apparent stability for the phase-separated emulsions. The stable compositions that can be formed provide potential for commercial applications in a number of areas. These would necessarily be based on this understanding of the role of the stabilizer as a part of a network and as surface active material, as it influences both mechanical and other properties.

Open Access Article. Published on 17 April 2025. Downloaded on 4/3/2026 5:41:20 PM. This article is licensed under a Creative Commons Attribution 3.0 Unported Licence.

Author contributions

Eleonora Olsmats: data curation, investigation, conceptualization, writing – original draft, writing – review & editing. Adrian R. Rennie: conceptualization, writing – original draft, writing – review & editing, funding acquisition. Daniel Bonn: conceptualization, writing – original draft, writing – review & editing, funding acquisition.

Data availability

Data for this article, including images and data sets are available at Zenodo at **https://doi.org/10.5281/zenodo.14724470**.

Conflicts of interest

There are no conflicts to declare.

Acknowledgements

This work was supported by the European Union's Horizon 2020 research and innovation programme under the Marie Skłodowska Curie PICKFOOD project, grant agreement No. 956248. EO wishes to thank the Institute of Physics at University of Amsterdam for hospitality during the study. The authors thank Marie Corpart, Paul Kolpakov and Elham Mirzahossein for assisting with the rheology and confocal microscopy experiments. The authors acknowledge the Department of Medicinal Chemistry at Uppsala University for access to the SAXS instrument.

Notes and references

1 T. F. Tadros, *Emulsion Formation and Stability*, Wiley-VCH Verlag GmbH & Co. KGaA, Weinheim, 2013.
2 S. U. Pickering, Emulsions, *J. Chem. Soc.*, 1907, **91**, 2001–2021.
3 W. Ramsden, Separation of solids in the surface-layers of solutions and 'suspensions' (observations on surface-membranes, bubbles, emulsions, and mechanical coagulation)—Preliminary Account, *Proc. R. Soc. London*, 1903, **72**, 156–164.
4 R. I. Dekker, S. F. Velandia, H. V. M. Kibbelaar, A. Morcy, V. Sadtler, T. Roques-Carmes, J. Groenewold, W. K. Kegel, K. P. Velikov and D. Bonn, Is there a difference between surfactant-stabilised and Pickering emulsions?, *Soft Matter*, 2023, **19**(10), 1941–1951.
5 S. Lam, K. P. Velikov and O. D. Velev, Pickering stabilization of foams and emulsions with particles of biological origin, *Curr. Opin. Colloid Interface Sci.*, 2014, **19**(5), 490–500.
6 J. Ge, C.-X. Sun, H. Corke, K. Gul, R.-Y. Gan and Y. Fang, The health benefits, functional properties, modifications, and applications of pea (*Pisum sativum* L.) protein: Current status, challenges, and perspectives, *Compr. Rev. Food Sci. Food Saf.*, 2020, **19**(4), 1835–1876.
7 E. Olsmats and A. R. Rennie, Pea protein [*Pisum sativum*] as stabilizer for oil/water emulsions, *Adv. Colloid Interface Sci.*, 2024, **326**, 103123.
8 Y. Shao and C.-H. Tang, Gel-like pea protein Pickering emulsions at pH 3.0 as a potential intestine-targeted and sustained-release delivery system for β-carotene, *Food Res. Int.*, 2016, **79**, 64–72.
9 H.-N. Liang and C.-H. Tang, Pea protein exhibits a novel Pickering stabilization for oil-in-water emulsions at pH 3, *LWT–Food Sci. Technol.*, 2014, **58**(2), 463–469.
10 X.-L. Li, W.-J. Liu, B.-C. Xu and B. Zhang, Simple method for fabrication of high internal phase emulsions solely using novel pea protein isolate nanoparticles: Stability of ionic strength and temperature, *Food Chem.*, 2022, **370**(4), 130899.
11 C. Sun, J.-J. Fu, Z.-F. Tan, G.-Y. Zhang, X.-B. Xu and L. Song, Improved thermal and oxidation stabilities of pickering high internal phase emulsions stabilized using glycated pea protein isolate with glycation extent, *LWT–Food Sci. Technol.*, 2022, **162**, 113465.
12 S. Sridharan, M. B. J. Meinders, J. H. Bitter and C. V. Nikiforidis, On the Emulsifying Properties of Self-Assembled Pea Protein Particles, *Langmuir*, 2020, **36**(41), 12221–12229.
13 P. Zhu, Y. Chu, J. Yang and L. Chen, Thermally reversible emulsion gels and high internal phase emulsions based solely on pea protein for 3D printing, *Food Hydrocolloids*, 2024, **157**, 110391.
14 B. P. Binks, Particles as surfactants - similarities and differences, *Curr. Opin. Colloid Interface Sci.*, 2002, **7**(1–2), 21–41.
15 M. Dinkgreve, K. P. Velikov and D. Bonn, Stability of LAPONITE®-stabilized high internal phase Pickering emulsions under shear, *Phys. Chem. Chem. Phys.*, 2016, **18**(33), 22973–22977.
16 E. Olsmats and A. R. Rennie, Understanding Stabilization of Oil-in-Water Emulsions with Pea Protein - Studies of Structure and Properties, *Langmuir*, 2024, **40**(26), 13386–13396.
17 E. Olsmats, R. P. Ravindranathan, K. D. Knudsen, J. Kohlbrecher, D. Bonn and A. R. Rennie, Emulsions stabilized by pea protein – hydration and protein distribution, *Food Hydrocolloids*, 2025, **162**, 110989.
18 M. Xu, W. Zhang, J. Jiang, X. Pei, H. Zhu, Z. Cui and B. P. Binks, Transition between a Pickering Emulsion and an Oil-in-Dispersion Emulsion Costabilized by Alumina Nanoparticles and a Cationic Surfactant, *Langmuir*, 2020, **36**(51), 15543–15551.
19 M. R. Bittermann, M. Grzelka, S. Woutersen, A. M. Brouwer and D. Bonn, Disentangling Nano- and Macroscopic Viscosities of Aqueous Polymer Solutions Using a Fluorescent Molecular Rotor, *J. Phys. Chem. Lett.*, 2021, **12**(12), 3182–3186.
20 S. F. Velandia, M. R. Bittermann, E. Mirzahossein, G. Giubertoni, F. Caporaletti, V. Sadtler, P. Marchal, T. Roques-Carmes, M. B. J. Meinders and D. Bonn, Probing interfaces of pea protein-stabilized emulsions with a fluorescent molecular rotor, *Front. Soft Matter*, 2023, **3**, 1093168.
21 J. Kim and M. Lee, Excited-State Photophysics and Dynamics of a Hemicyanine Dye in AOT Reverse Micelles, *J. Phys. Chem. A*, 1999, **103**, 3378–3382.

 This journal is © The Royal Society of Chemistry 2025

Open Access Article. Published on 17 April 2025. Downloaded on 4/3/2026 5:41:20 PM. This article is licensed under a Creative Commons Attribution 3.0 Unported Licence.

22 Leica Application Suite X (LAS X), Leica Microsystems, [Online]. Available: https://www.leica-microsystems.com/products/microscope-software/p/leica-las-x-ls/. [Accessed 22 April 2024].
23 C. A. Schneider, W. S. Rasband and K. W. Eliceiri, NIH Image to ImageJ: 25 years of image analysis, *Nat. Methods*, 2012, **9**(7), 671–675.
24 XSACT, Xenocs, [Online]. Available: https://www.xenocs.com/saxs-products/xsact-software/. [Accessed 22 April 2024].
25 F. Zhang, J. Ilavsky, G. G. Long, J. P. G. Quintana, A. J. Allen and P. R. Jemian, Glassy Carbon as an Absolute Intensity Calibration Standard for Small-Angle Scattering, *Metall. Mater. Trans. A*, 2010, **41**, 1151–1158.
26 A. Mota da Silva, F. Souza Almeida and A. C. Kawazoe Sato, Functional characterization of commercial plant proteins and their application on stabilization of emulsions, *J. Food Eng.*, 2021, **292**, 110277.
27 F. Zhan, X. Tang, R. Sobhy, B. Li and Y. Chen, Structural and rheology properties of pea protein isolate-stabilized emulsion gel: Effect of crosslinking with transglutaminase, *Int. J. Food Sci. Technol.*, 2022, **57**(2), 974–982.
28 K. Grasberger, A. Vuholm Sunds, K. Wejse Sanggaard, M. Hammershøj and M. Corredig, Behavior of mixed pea-whey protein at interfaces and in bulk oil-in-water emulsions, *Innovative Food Sci. Emerging Technol.*, 2022, **81**, 103136.
29 A. C. Karaca, N. Low and M. Nickerson, Emulsifying properties of chickpea, faba bean, lentil and pea proteins produced by isoelectric precipitation and salt extraction, *Food Res. Int.*, 2011, **44**(9), 2742–2750.
30 R. E. Aluko, M. A. Olawunmi and B. M. Watts, Emulsifying and Foaming Properties of Commercial Yellow Pea (*Pisum sativum* L.) Seed Flours, *J. Agric. Food Chem.*, 2009, **57**, 9793–9800.
31 M. L'Estimé, M. Schindler, N. Shahidzadeh and D. Bonn, Droplet Size Distribution in Emulsions, *Langmuir*, 2024, **40**(1), 275–281.
32 L. Chang, Y. Lan, B. Chen and J. Rao, Interfacial, and emulsifying properties nexus of green Pea protein fractions: Impact of pH and salt, *Food Hydrocolloids*, 2023, **140**, 108652.
33 K. F. Grasberger, F. Wendelboe Lund, A. Cohen Simonsen, M. Hammershøj, P. Fischer and M. Corredig, Role of the pea protein aggregation state on their interfacial properties, *J. Colloid Interface Sci.*, 2024, **658**, 156–166.
34 V. Ducel, J. Richard, Y. Popineau and F. Boury, Adsorption Kinetics and Rheological interfacial Properties of Plant Proteins at the Oil-Water Interface, *Biomacromolecules*, 2004, **5**(6), 2088–2093.
35 M. T. Hossain and R. H. Ewoldt, Protorheology, *J. Rheol.*, 2024, **68**, 113–144.
36 E. L. Hansen, H. Hemmen, D. M. Fonseca, C. Coutant, K. D. Knudsen, T. S. Plivelic, D. Bonn and J. O. Fossum, Swelling transition of a clay induced by heating, *Sci. Rep.*, 2012, **2**(1), 618.
37 D. Bonn, M. M. Denn, L. Berthier, T. Divoux and S. Manneville, Yield stress materials in soft condensed matter, *Rev. Mod. Phys.*, 2017, **89**(3), 035005.
38 S. Zhang, J. Han and L. Chen, Fabrication of pea protein gels with modulated rheological properties using high pressure processing, *Food Hydrocolloids*, 2023, **144**, 109002.
39 D. Chen, I. Kuzmenko, J. Ilavsky, L. Pinho and O. Campanella, Structural evolution during gelation of pea and whey proteins envisaged by time-resolved ultra-small-angle x-ray scattering (USAXS), *Food Hydrocolloids*, 2022, **126**, 107449.
40 R. Kornet, J. Yang, P. Venema, E. van der Linden and L. M. C. Sagis, Optimizing pea protein fractionation to yield protein fractions with a high foaming and emulsifying capacity, *Food Hydrocolloids*, 2022, **126**, 107456.
41 A. Kimura, T. Fukuda, M. Zhang, S. Motoyama, N. Maruyama and S. Utsumi, Comparison of Physicochemical Properties of 7S and 11S Globulins from Pea, Fava Bean, Cowpea, and French Bean with Those of Soybean—French Bean 7S Globulin Exhibits Excellent Properties, *J. Agric. Food Chem.*, 2008, **56**(21), 10273–10279.
42 S. Sacanna, W. K. Kegel and A. P. Philipse, Thermodynamically Stable Pickering Emulsions, *Phys. Rev. Lett.*, 2007, **98**, 158301.
43 D. J. Kraft, J. W. J. de Folter, B. Luigjes, S. I. R. Castillo, S. Sacanna, A. P. Philipse and W. K. Kegel, Conditions for Equilibrium Solid-Stabilized Emulsions, *J. Phys. Chem. B*, 2010, **114**(32), 10347–10356.